Cancer Letters 450 (2019) 155–168

Contents lists available at ScienceDirect

Cancer Letters

journal homepage: www.elsevier.com/locate/canlet

Original Articles

Insulin receptor isoform A favors tumor progression in human hepatocellular carcinoma by increasing stem/progenitor cell features

Eva Benabou[a], Zeina Salamé[a], Dominique Wendum[a,b,c], Marie Lequoy[a,d], Sylvana Tahraoui[a], Fatiha Merabtene[c], Yves Chrétien[a], Olivier Scatton[a,e], Olivier Rosmorduc[a,f], Laura Fouassier[a], Laetitia Fartoux[a,f], Françoise Praz[a], Christèle Desbois-Mouthon[a,*]

[a] Sorbonne Université, INSERM, Saint-Antoine Research Center, F-75012, Paris, France
[b] AP-HP, Saint-Antoine HCospital, Department of Pathology, F-75012, Paris, France
[c] Histomorphology Platform, UMS 30 Lumic, F-75012, Paris, France
[d] AP-HP, Saint-Antoine Hospital, Department of Hepatology, F-75012, Paris, France
[e] AP-HP, Pitié-Salpétrière Hospital, Department of Hepatobiliary Surgery and Liver Transplantation, F-75013, Paris, France
[f] AP-HP, Pitié-Salpétrière Hospital, Department of Hepatology, F-75013, Paris, France

ARTICLE INFO

Keywords:
Liver cancer
INSR
Invasion
Cytokeratin-19

ABSTRACT

Hepatocellular carcinoma (HCC) is one of the most common and deadly neoplasms. Insulin receptor (IR) exists in two isoforms, IR-A and IR-B, the latter being predominantly expressed in normal adult hepatocytes while IR-A is overexpressed in HCC to the detriment of IR-B. This study evaluated the biological functions associated with IR-A overexpression in HCC in relation to expression of its ligand IGF-II. The value of *INSRA:INSRB* ratio which was increased in ~70% of 85 HCC was associated with stem/progenitor cell features such as cytokeratin-19 and α-fetoprotein and correlated with shorter patient survival. *IGF2* mRNA upregulation was observed in 9.4% of HCC and was not associated with higher *INSRA:INSRB* ratios. Ectopic overexpression of IR-A in two HCC cell lines presenting a strong autocrine IGF-II secretion loop or not stimulated cell migration and invasion. In cells cultured as spheroids, IR-A overexpression promoted gene programs related to stemness, inflammation and cell movement. IR-A also increased cell line tumorigenicity *in vivo* after injection to immunosuppressed mice and the sphere-forming cells made a significant contribution to this effect. Altogether, these results demonstrate that IR-A is a novel player in HCC progression.

1. Introduction

Hepatocellular carcinoma (HCC) is the second cause of cancer-related death worldwide and the fifth most common malignancy [1]. HCC is induced by multiple etiologies and exhibits substantial heterogeneity, which complicates the development of effective therapies. HCC harboring stem/progenitor cell features are of poorer outcome [2]. Despite advances in the molecular and genetic profiling, the molecular pathogenesis of HCC is still not fully understood. Due to the expected increase in HCC incidence within the next years which will be mostly driven by obesity and diabetes [3], studies on the molecular checkpoints involved in HCC progression and aggressiveness represent an important issue.

The insulin receptor (IR) tyrosine kinase (TK) exists in two isoforms, IR-A and IR-B, due to alternative splicing of exon 11 encoding 12 amino acids located at the carboxy-terminal domain of extracellular subunits. IR-B (long form) is mainly expressed in insulin target cells, *i.e* adult hepatocytes, skeletal muscle cells and adipocytes. IR-B binds only insulin at physiological concentrations and especially conveys hormone effects on glucose and lipid metabolism. IR-A (short form) is the predominant isoform expressed during fetal development and binds not only insulin but also insulin-like growth factor-II (IGF-II) with high affinity [4]. Up-regulation of *INSRA* has been observed in a variety of human cancer cell lines and tumors [5]. In HCC, we previously reported that *INSRA* is frequently upregulated to the detriment of *INSRB* thus raising the *INSRA:INSRB* expression ratio [6,7]. The expression shift from *INSRB* towards *INSRA* was related to epidermal growth factor (EGF) receptor-mediated dysregulation of specific RNA splicing factors favoring exon 11 exclusion from *INSR* pre-mRNA [6]. In addition, we recently showed that the expression levels of *INSRA* mRNA in an experimental model of HCC reflect plasma levels of IR-A suggesting that the measurement of circulating IR-A may assist HCC management [8]. The role of IR-A in HCC remains to be elucidated.

* Corresponding author. INSERM UMR_S938, Centre de Recherche Saint-Antoine, 34 rue Crozatier, 75012, Paris, France.
E-mail address: christele.desbois-mouthon@inserm.fr (C. Desbois-Mouthon).

https://doi.org/10.1016/j.canlet.2019.02.037
Received 28 August 2018; Received in revised form 9 December 2018; Accepted 15 February 2019

Abbreviations

AFP	α-fetoprotein
CK19	cytokeratin 19
EGF	epidermal growth factor
EMT	epithelial-mesenchymal transition
GFP	green fluorescent protein
GSEA	gene set enrichment analysis
CC	hepatocellular carcinoma
IF	immunofluorescence
IHC	immunohistochemistry
IPA	ingenuity pathway analysis
IR	insulin receptor
IGF1R	insulin-like growth factor-I receptor
IGF-II	insulin-like growth factor-II
qPCR	quantitative real-time PCR
RT	reverse transcription
SEM	standard error of the mean
TGF	transforming growth factor
TK	tyrosine kinase

At the molecular level, IR-A is thought to signal in response to IGF-II as some malignant cells exhibit both autocrine production of IGF-II and IR-A overexpression [9–11]. The consequences of IGF-II/IR-A expression on cancer cell biology have been investigated mainly *in vitro* and were essentially focused on proliferation and invasion such as in leiomyosarcoma [12] and prostate cancer cells [13]. There is a need to extend these findings to human tumors by examining whether IR-A expression is associated to aggressiveness markers in tumors and bad prognosis in patients with cancer.

Interestingly, the last years have seen renewed interest for the study of IR-A signaling in cancer. Indeed, elevated expression as well as compensatory activation of IR-A have been identified as intrinsic and adaptive resistance mechanisms to IGF1 receptor (IGF1R) therapies [14–18]. To overcome this problem, therapeutic strategies targeting IGF-II, a ligand common to IR-A and IGF1R, are currently under clinical investigation. The recent pre-clinical evaluation of a neutralizing antibody against IGF-II provided encouraging results in HCC [19].

In this context, the aim of the present study was to define the contribution of IR-A-dependent signaling to HCC progression. We examined the relationship between IR-A and IR-B expression and the clinicopathological features of HCC and studied the impact of ectopic overexpression of IR-A or IR-B on HCC cell biology using human cell lines possessing a strong autocrine IGF-II loop or not.

2. Materials and methods

2.1. Patients and human liver tissue specimens

HCC and paired non-tumor liver tissues were collected from 85 patients who underwent curative liver resection. The clinicopathological characteristics have been published elsewhere [7]. All patients gave informed consent to the study, which was conducted in accordance with the French laws and regulations (CNIL n° 1913901 v 0).

2.2. Cell culture and treatments

Huh7 cells were obtained from the American Type Culture Collection. PLC/PRF5 cells were provided by Dr Christine Perret (Institut Cochin, France). Cell lines were authenticated using short tandem repeats as described [20], cultured as previously reported [21] and routinely controlled for *mycoplasma* contamination. In some experiments, serum-deprived cells were treated with insulin, IGF-II (Sigma-Aldrich) or TGF-β1 (Preprotech). HCC cell lines were transfected with plasmids expressing human IR-A (pRcCMVi.hIR-A (GFP)) or

Table 1
Relations between IR-A:IR-B fold inductions (T/NT) and the pathological characteristics of 85 HCC.

	n	IR-A:IR-B fold induction (T/NT)[a]	P values
HBV			
yes	27	2.38 [1.09–18.47]	0.639
no	58	2.71 [0.07–39.30]	
HCV			
yes	21	3.25 [0.35–39.30]	0.409
no	64	2.54 [0.07–19.75]	
NASH			
yes	11	2.68 [0.95–12.76]	0.773
no	74	2.54 [0.07–39.30]	
MS + alcohol			
yes	8	1.83 [0.90–5.16]	0.166
no	77	2.65 [0.07–39.30]	
Alcohol			
yes	5	3.00 [1.74–3.14]	0.971
no	80	2.54 [0.07–39.30]	
Advanced fibrosis/cirrhosis			
yes	50	2.22 [0.70–39.30]	0.138
no	35	3.18 [0.07–19.75]	
AFP[b]			
< 400 ng/mL	47	2.11 [0.07–39.30]	**0.002**
≥ 400 ng/mL	34	3.93 [0.74–19.17]	
Tumor size			
< 5 cm	44	2.20 [0.07–39.30]	0.105
≥ 5 cm	41	3.05 [0.35–19.75]	
Multiplicity			
yes	18	2.77 [0.07–19.17]	0.817
no	67	2.54 [0.35–39.30]	
Satellite nodules			
yes	26	3.00 [1.09–19.75]	0.366
no	59	2.52 [0.35–39.30]	
Differentiation			
well/moderate	61	2.14 [0.07–19.75]	< **0.0001**
poor	24	5.35 [0.74–39.30]	
CK19 expression[c]			
< 5%	65	2.22 [0.07–19.75]	**0.002**
≥ 5%	17	5.54 [0.35–39.30]	
Microvascular invasion			
yes	41	3.05 [0.07–19.75]	**0.023**
no	44	2.13 [0.37–39.30]	

AFP: α-fetoprotein; CK19: cytokeratin 19; HCV: hepatitis C virus; HBV, hepatitis B virus; MS, metabolic syndrome; NASH, nonalcoholic steatohepatitis.
All statistical analyses were performed using a Mann-Whitney test.
[a] Values are expressed as median [range].
[b] Four missing data.
[c] Three missing data.

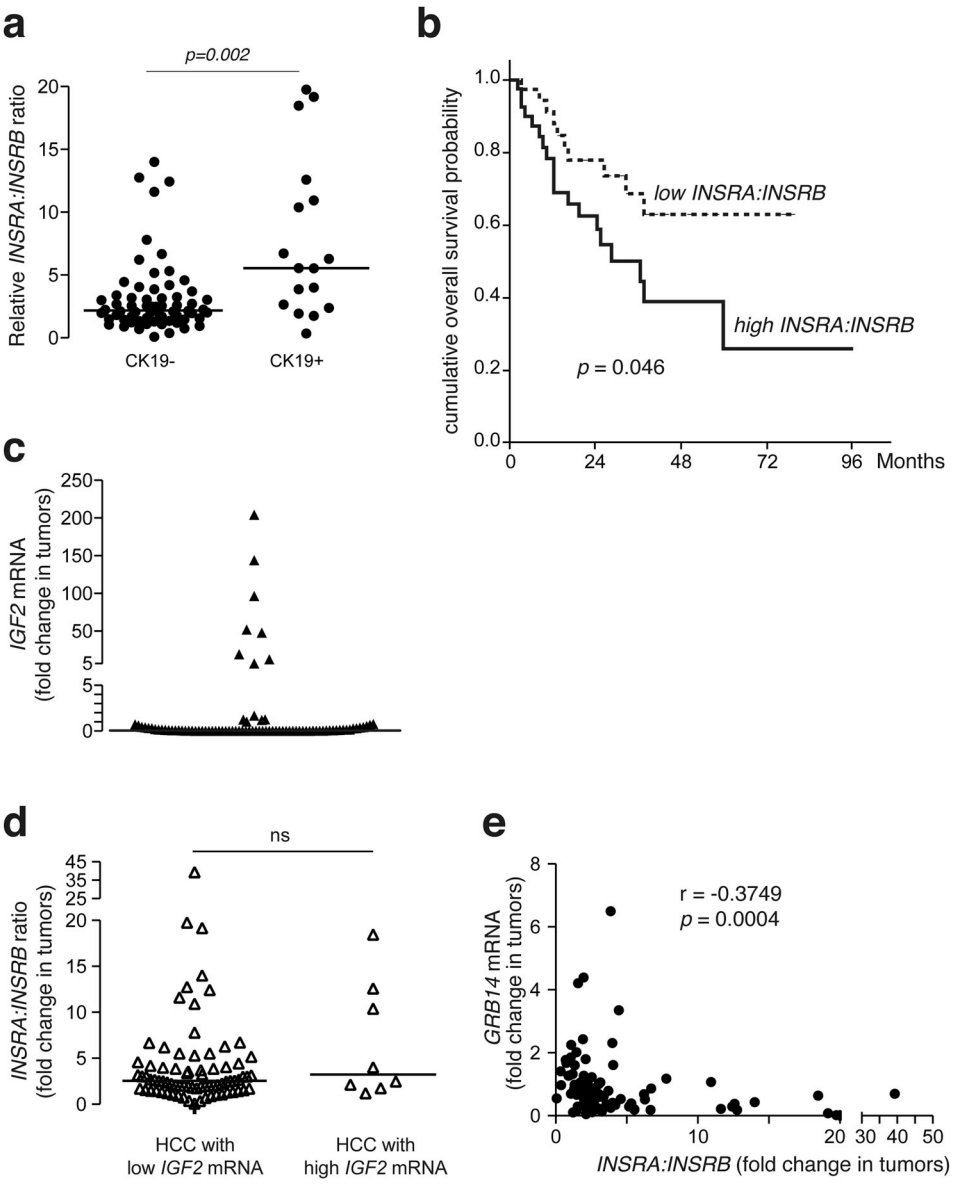

Fig. 1. Status of IR-A signaling in human HCC. a. The fold changes of *INSRA*:*INSRB* ratio were assigned into two subgroups according to IHC detection of CK19 (< 5% ($CK19^-$) or > 5% ($CK19^+$) of cells). **b.** Kaplan-Meier analysis comparing overall survival of 85 patients with HCC according to the median value of the *INSRA*:*INSRB* ratio. **c.** Expression of *IGF2* mRNA was measured by RT-qPCR. Each dot represents the fold change in HCC *versus* paired nontumor tissue (n = 85). **d.** The fold changes of *INSRA*:*INSRB* ratio were assigned into two subgroups according to the level of expression of *IGF2* mRNA. **e.** Correlation between *GRB14* mRNA and *INSRA*:*INSRB* ratio levels in 85 HCC. Black lines are the medians. ns, not significant.

IR-B (pRcCMVi.hIR-B (GFP)) fused to green fluorescent protein (GFP) [22–26] using Lipofectamine™ 3000 and selected with G418 (ThermoFisher Scientific). After two rounds of selection based on GFP expression by flow cytometry cell sorting (MoFlo® Astrios™, Beckman Coulter), pools of stably transfected cell lines were established.

2.3. Xenografts

Mice were maintained in accordance with the French guidelines for the humane treatment and care of laboratory animals (agreement N° 01350.02). Subcutaneous xenografts were performed in 5-weeks old female nude (Hsd:athymic Nude-Foxn1^{nu}, Envigo) and NOD/SCID (NOD.Cg-Prkdc^{scid} Il2rg^{tm1Wjl}/SzJ, Charles River) mice as reported elsewhere [21].

2.4. Immunoblotting

Protein electrophoresis and transfer to nitrocellulose were performed according to standard procedures. The primary antibodies are summarized in Supplementary Table S1. Blot quantifications were performed using ChemiDoc™ Touch Imaging System (BioRad). The phosphorylation status of 42 human RTKs was determined by Proteome Profiler™ array (R&D Systems).

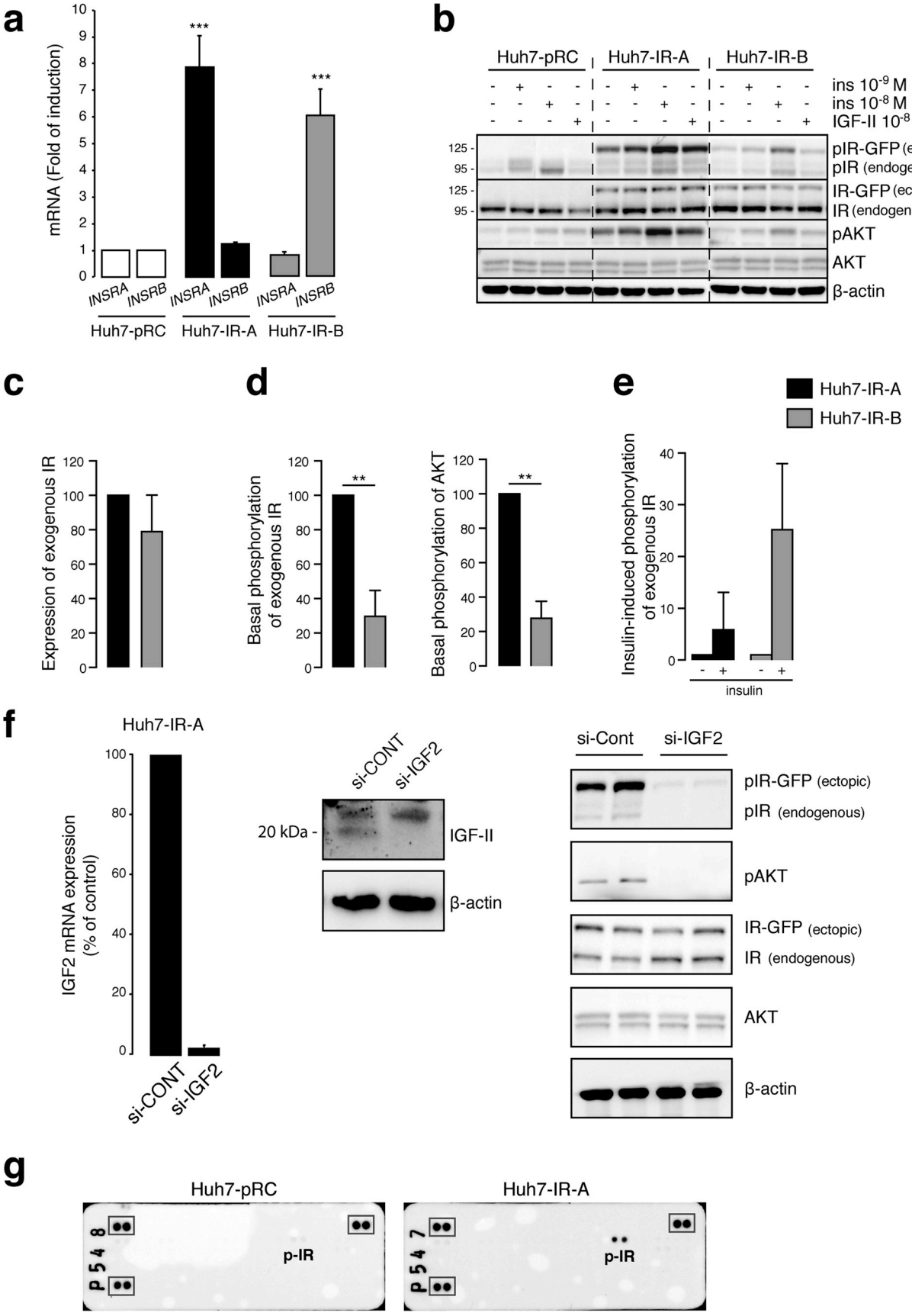

(caption on next page)

Fig. 2. Characterization of Huh7 cell lines overexpressing IR-A or IR-B. **a.** *INSR*A and *INSRB* mRNA expression was measured by RT-qPCR in Huh7 cells stably expressing the empty plasmid (Huh7-pRC, n = 4), IR-A-GFP cDNA (Huh7-IR-A, n = 4), or IR-B-GFP cDNA (Huh7-IR-B, n = 4). Fold change is normalized to control Huh7-pRC cells. **b.** Western blot analysis of stably transfected Huh7 pools stimulated with or without insulin or IGF-II. β-actin was used as a loading control. Ectopic receptors fused to GFP (IR-GFP) have an apparent molecular weight of 125 kDa. **c.** Blot quantifications showing the ratio of total ectopic IR to β-actin level (n = 3). **d.** Blot quantifications showing the ratio of phosphorylated to total ectopic IR (*left panel*) and AKT (*right panel*) level (n = 3). **e.** Blot quantifications showing the effect of insulin (10^{-8} M, 10 min) on ectopic IR activation (ratio of phosphorylated to total) (n = 3). **f.** Huh7-IR-A cells were treated with siRNA against *IGF2* (si-IGF2) or with control siRNA (si-CONT) and expression of *IGF2* was measured by RT-qPCR (n = 2) (*left panel*) and Western blot (*middle panel*). The impact of *IGF2* downregulation was examined by Western blot analysis on IR and AKT phosphorylation (n = 2) (*right panel*). **g.** RTK profiler array showing IR tyrosine phosphorylation in Huh7-pRC and Huh7-IR-A cells cultured in serum-deprived medium for 24 h. Corner boxes delineate control spots. Representative blots of two or three independent experiments are shown. Values are mean ± SEM. $*p < 0.05$, $**p < 0.01$, $***p < 0.001$.

2.5. RNA interference

The expression of *IGF2* mRNA was downregulated using a mixture of four siRNAs (ON-TARGET*plus*™ SMARTpool) and DharmaFECT® 4 transfection reagent. Control experiments were performed using a non-targeting siRNA pool (Dharmacon).

2.6. RNA isolation, reverse transcription (RT) and quantitative real-time PCR (qPCR)

RNA isolation, RT and qPCR using specific primers (Supplementary Table S2) were performed as reported elsewhere [6].

2.7. Immunohistochemistry (IHC)

Paraffin-embedded 4-µm sections were dewaxed in xylene and rehydrated in graded alcohol series and antigen retrieval was performed in EDTA pH 9.0 during 15 min at 95 °C. Primary antibody (1:30, 30 min, Supplementary Table S1) was detected using Novolink Polymer Detection System (Leica Biosystems). Aminoethyl carbazole was used to reveal the peroxidase activity (Vector laboratories). The sections were counterstained with haematoxylin.

2.8. Proliferation assay

Twenty thousand cells were seeded in triplicate in 24-well plates and cell numbers were evaluated 48, 72 and 96 h later.

2.9. Migration and invasion assays

Migration and invasion assays were performed in Transwells® (Corning) with 8-µm pore polycarbonate membrane insert coated (invasion) or not (migration) with Matrigel® as reported previously [27].

2.10. Sphere formation assay

One thousand cells were plated onto ultra-low attachment 6-well plates (Corning) and cultured in DMEM/F12 medium with B27 supplement, 20 ng/mL EGF, 20 ng/mL basic fibroblast growth factor and 100 µg/mL gentamycin (Life Technologies) during 14 days.

2.11. Immunofluorescence (IF)

Hepatospheres were fixed with 4% paraformaldehyde, permeabilized with 0.2% Triton X-100, blocked with 3% BSA and 10% goat serum in PBS, followed by an overnight incubation with the primary antibody (1:50 dilution) in PBS at 4 °C (Supplementary Table S1). Spheres were then incubated with a 1:200 dilution of conjugated secondary antibody (Alexa Fluor® 546 dye) in PBS for 1 h at room temperature, washed and incubated with 4′,6-diamidino-2-phenylindole (DAPI) for nucleus staining.

2.12. Transcriptome analysis

Gene expression profiles from three tumors/spheres derived from Huh7 cells stably expressing the empty construct or pRcCMVi.hIR-A (GFP) were analyzed using GeneChip™ human gene 2.0 ST array (Affymetrix). Datasets are available at GSE111707. Gene set enrichment analysis (GSEA) [28] was performed using the MSigDB hallmark gene set collection and C2 collection of curated gene sets. Ingenuity pathway analysis (IPA) software (Ingenuity Systems) was used to identify top biological functions and networks.

2.13. Statistical analyses

Statistical analyses were performed using SPSS software (IBM Corp.) or GraphPad Prism (GraphPad Software, Inc.). When data sets met normal distribution criteria, two-sided Student *t*-test analysis (for two-group comparisons) and one-way analysis of variance (if more than two groups were compared) were used. A Bonferroni test was used as a post-hoc test. If data did not meet normal distribution criteria, Mann–Whitney *U* test (for two-group comparisons) and Kruskal–Wallis test (if more than two groups were compared) were used. A Dunn's test was used as a post-hoc test. Survival analysis was done by the Kaplan–Meier method and the two groups were compared with the log-rank test. Correlations between mRNA expression levels were conducted using Spearman rank correlation coefficient. Data from *in vitro* experiments are reported as mean ± standard error of the mean (SEM) of at least three independent experiments. Differences were considered statistically significant at $p < 0.05$.

3. Results

3.1. A high INSRA:INSRB ratio is associated with clinicopathological markers of HCC aggressiveness

We previously reported that the *INSRA*:*INSRB* ratio was increased in ~70% of HCC [6,7]. Here we examined whether aberrant expression of IR isoforms was linked to specific clinicopathological characteristics. No significant association was found between the *INSRA*:*INSRB* ratio in

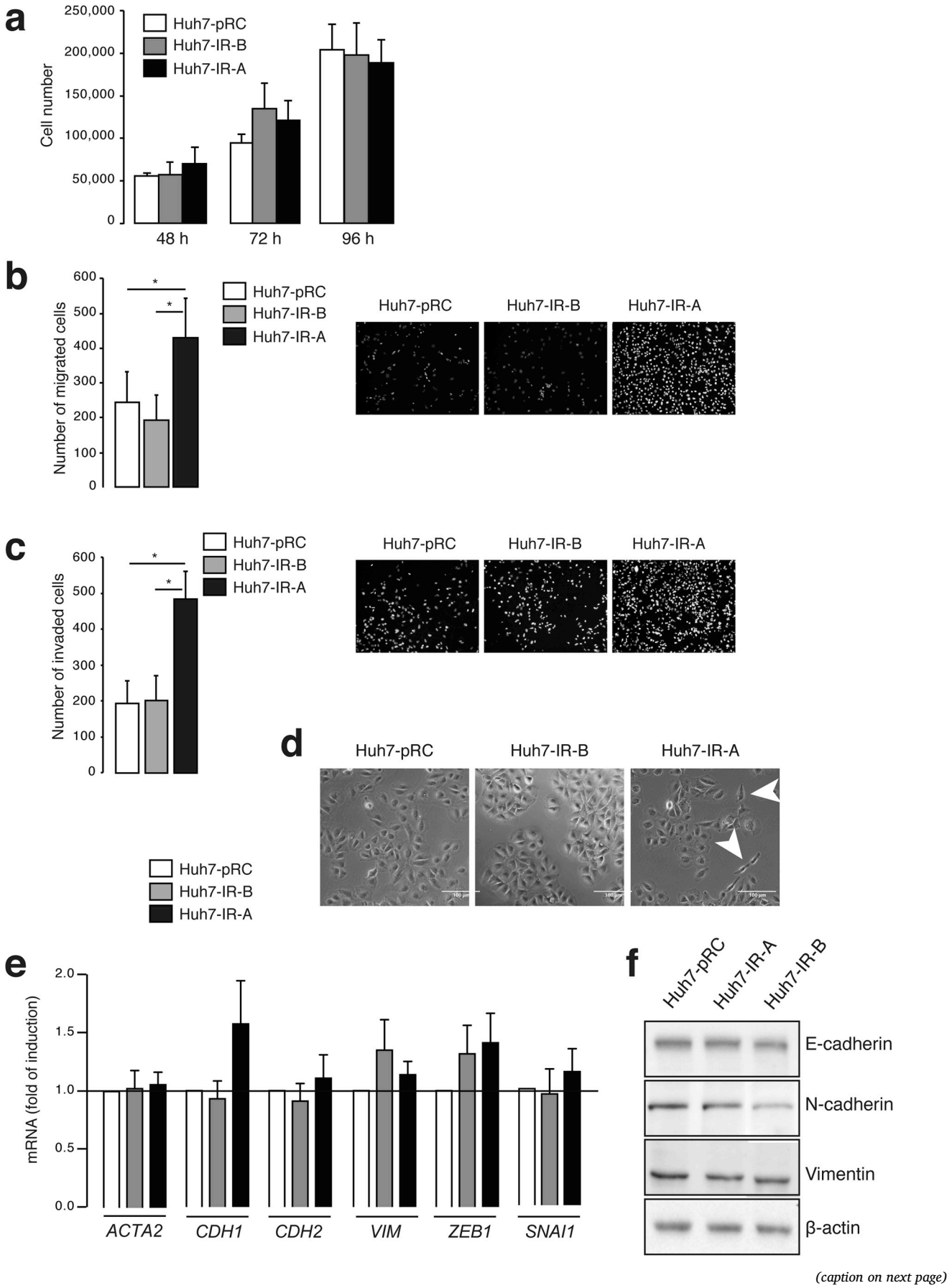

(caption on next page)

Fig. 3. Effects of IR-A overexpression on migration and invasion of Huh7 cells *in vitro*. **a.** Cell number was evaluated 48 h, 72 h and 96 h after plating (n = 4). **b.** Cell migration was measured 30 h after plating using Transwell® inserts (n = 6). Representative pictures of migrated cells stained with DAPI are shown on the right. **c.** Cell invasion was measured 30 h after plating using Transwell® inserts coated with Matrigel® (n = 7). Representative pictures of invaded cells stained with DAPI are shown on the right. **d.** Microscopic examination of cell morphology. Arrows indicate individually scattered cells. **e.** Expression of *ACTA2*, *CDH1, CDH2, VIM, ZEB1, and SNAI1* mRNA was measured by RT-qPCR in Huh7-pRC (n = 5), Huh7-IR-A (n = 5) and Huh7-IR-B (n = 4) cells. **f.** Western blot analysis of stably transfected Huh7 pools for EMT markers. β-actin was used as a loading control (representative pictures; n = 3). Values are mean ± SEM. $*p < 0.05$.

HCC and the different etiologies (Table 1). In contrast, a high *INSRA*:*INSRB* ratio was associated with histological and biological markers reminiscent of tumors with poor outcome such as poor differentiation, microvascular invasion, high serum levels of α-fetoprotein (AFP), and expression of cytokeratin 19 (CK19), the two latter being validated biomarkers for HCC with hepatic progenitor cell features (Table 1, Fig. 1a). Moreover, patients with a high *INSRA*:*INSRB* ratio had a significant shorter overall survival after curative resection (Fig. 1b). Of note, no association with clinicopathological characteristics was observed when total *INSR* gene expression was considered (data not shown). The examination of the status of the high affinity ligand IGF-II showed a bimodal distribution of *IGF2* mRNA fold change in tumors with only eight specimens out of 85 (9.4%) having a fold-change ≥ 7 (Fig. 1c). Most of these tumors were CK19 and AFP positive tumors (Supplementary Table S3). There was no association between *INSRA*:*INSRB* ratio and *IGF2* expression level (Fig. 1d). Thus, the deregulation of *INSRA*:*INSRB* ratio is more common than the overexpression of *IGF2* in HCC. Finally, we observed an inverse relationship between *INSRA*:*INSRB* ratio and mRNA encoding GRB14, a physiological negative regulator of IR TK activity that we recently reported to be frequently down-regulated in HCC [7] (Fig. 1e).

3.2. Ectopic overexpression of IR-A increases migration and invasion in Huh7 cells with IGF-II autocrine loop

To examine how IR-A impacts the biology of HCC cells, we generated pools of Huh7 cells stably overexpressing human IR-A (Huh7-IR-A), IR-B (Huh7-IR-B) or the empty vector (Huh7-pRC). Huh7 cells possess a strong autocrine production of IGF-II (Supplementary Fig. S1). Each IR isoform was tagged with monomeric GFP fused to the C-terminal domain of the β-subunit. The addition of monomeric GFP was reported to have no impact on IR synthesis and ligand-mediated activation and signaling [22–26]. RT-qPCR (Fig. 2a) and Western blotting (Fig. 2b and c) confirmed that chimeric IR were expressed to similar and physiological levels in Huh7-IR-A and Huh7-IR-B cells. Basal phosphorylation of IR-GFP and AKT was increased in Huh7-IR-A cells compared to Huh7-IR-B cells (Fig. 2b,d) and resulted from IGF-II autocrine loop as phosphorylation was abolished by an *IGF2* siRNA (Fig. 2f). Endogenous IR which was mainly IR-B isoform in this cell line [6] was activated by insulin. IGF-II had no effect on IR-GFP phosphorylation in Huh7-IR-B cells while insulin increased IR-GFP and AKT phosphorylation in these cells (Fig. 2b,e). Therefore, tagged IRs were efficiently expressed in Huh7 cells and retained their ability to undergo autophosphorylation and activate downstream signaling in response to their specific ligands. In addition, phospho-RTK array showed that IR was the sole RTK which was overactivated in Huh7-IR-A cells cultured in serum-free conditions (Fig. 2g).

We then studied the impact of ectopic overexpression of IR-A on proliferation, migration and invasion in Huh7 cells. We did not find evidence for increased cell proliferation in IR-A-overexpressing Huh7 cells as assessed by direct cell counting (Fig. 3a). In contrast, Huh7-IR-A cells displayed increased migratory and invasive properties while Huh7-IR-B cells behaved as control cells (Fig. 3b and c). *IGF2* siRNA reduced the invasive potential of Huh7-IR-A cells (Supplementary Fig. S2). These data led us to examine whether IR-A could regulate epithelial-mesenchymal transition (EMT). Microscopic examination showed that individually scattered cells were more frequent among Huh7-IR-A cells compared to Huh7-pRC cells and Huh7-IR-B cells (3.25 ± 0.55%, 0.56 ± 0.19% and 0.48 ± 0.17%, respectively; $p = 0.03$) (Fig. 3d). While Huh7-IR-A cells were able to undergo EMT under TGF-β1 treatment (Supplementary Fig. S3), the expression of EMT-related markers was unaltered in Huh7-IR-A cells compared to Huh7-pRC and Huh7-IR-B (Fig. 3e and f). Altogether these data indicate that ectopic overexpression of IR-A has marked effects on Huh7 cell biology *in vitro* by promoting cell migratory and invasive properties in response to autocrine IGF-II but independently of an EMT induction.

3.3. Ectopic overexpression of IR-A promotes the expression of cancer stem/progenitor cell (CSC) markers in Huh7 cells with IGF-II autocrine loop

As the *INSRA:INSRB* ratio was enriched in human tumors with CSC features (Table 1, Fig. 1a), we examined whether the ectopic overexpression of IR-A may affect cancer cell plasticity. CSCs can be enriched *in vitro* by culturing cancer cells as spheroids in non-adherent conditions [29,30]. We took advantage of this method to examine whether IR-A overexpression may affect the CSC contingent in Huh7 cells. As shown in Fig. 4a, the ability of Huh7-IR-A cells to form spheroids was similar to that of Huh7-pRC and Huh7-IR-B cells. However, Huh7-IR-A spheres were structures with irregular edges, comprising cohesive but loosely packed cells while control and Huh7-IR-B spheres were tightly packed and cohesive within a well-defined border (Fig. 4b). Huh7-pRC spheres expressed significantly higher levels of *INSRA* mRNA compared to adherent Huh7-pRC cells suggesting a potential role for IR-A in CSCs (Fig. 4c). The expression of ectopically expressed *INSR* isoforms was similar between Huh7-IR-A and Huh7-IR-B spheres (Fig. 4d). A comparative transcriptomic analysis followed by GSEA showed that Huh7-IR-A spheres were enriched in signatures related to stem cell/progenitor cells compared to Huh7-pRC spheres (Fig. 4e and Supplementary Fig. S4a). Using RT-qPCR, we observed that Huh7-IR-A spheres expressed higher levels of CSC markers including *KRT19* mRNA while Huh7-IR-B spheres showed a marked down-regulation of *KRT19* and *PROM1/CD133* expression in comparison with control spheres (Fig. 4f). The upregulation of CK19 was confirmed in Huh7-IR-A spheres by immunofluorescence (Fig. 4g). GSEA also identified significant enrichment of inflammatory signatures in Huh7-IR-A spheres (Supplementary Fig. S4b). Moreover, pathways related to

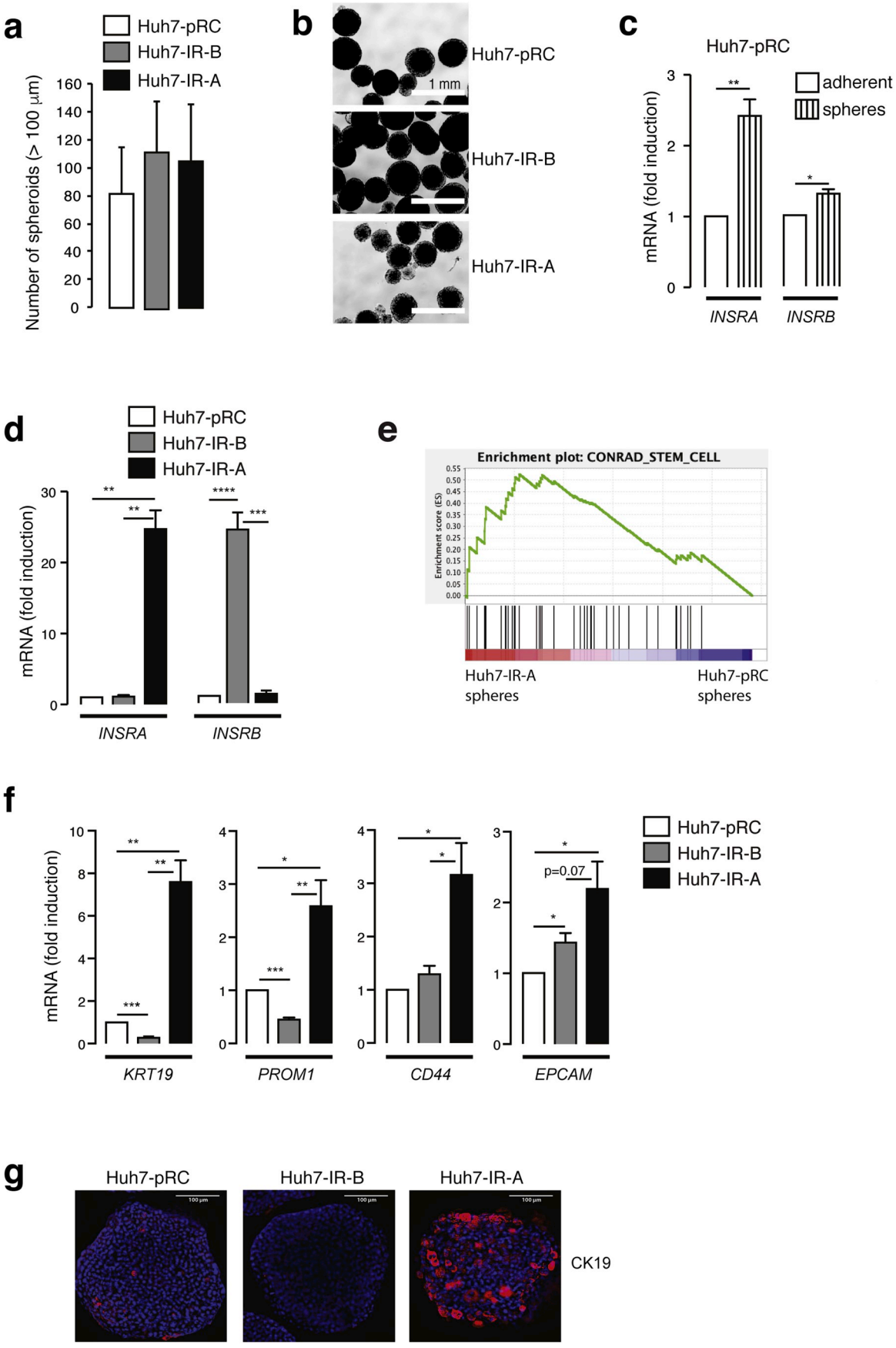

(caption on next page)

Fig. 4. Effects of IR-A overexpression on CSC contingent in Huh7 cells *in vitro*. **a.** Huh7-pRC, Huh7-IR-A and Huh7-IR-B cells were cultured in non-adherent conditions during 14 days and the number of hepatospheres (> 100 μm) was evaluated (n = 4). **b.** Representative pictures showing morphology of spheroids. **c.** Expression of *INSRA* and *INSRB* mRNA in Huh7-pRC cells cultured in adherent or non-adherent (spheres) conditions (n = 4). **d.** Comparative expression of *INSRA* and *INSRB* mRNA in spheres (n = 4). **e.** GSEA revealed an enrichment of progenitor signatures in Huh7-IR-A spheres such as CONRAD_STEM_CELL. **f.** Expression of *KRT19, PROM1, CD44 and EPCAM* mRNA was measured by RT-qPCR in spheres (n = 4). **g.** CK19 protein was detected by IF in hepatospheres. $^{*}p < 0.05$, $^{**}p < 0.01$, $^{***}p < 0.001$, $^{****}p < 0.0001$.

migration and invasion of cancer cells were up-regulated in Huh7-IR-A spheres (Supplementary Fig. S4c) which supported our previous *in vitro* data showing higher migratory and invasive potentials for Huh7-IR-A cells (Fig. 3b and c).

3.4. Ectopic overexpression of IR-A increases tumorigenicity of Huh7 cells with IGF-II autocrine loop

Next, we compared the propensity of the three cell lines to favor tumor development after subcutaneous injection of 2×10^6 cells to nude mice. Tumor appearance and growth were increased markedly with Huh7-IR-A compared with Huh7-pRC cells while tumors obtained from Huh7-IR-B cells behave as controls (Fig. 5a and Supplementary Table S4). To evaluate whether cells contained in Huh7-IR-A spheroids contributed to increased tumorigenesis, we injected as few as 1×10^3 spheroids-derived cells to NOD/SCID mice. As shown in Fig. 5b, 75% of mice injected with Huh7-IR-A spheroids developed tumors within 6 months (of note, one mouse from this group was not analyzed due to premature death from lymphoma) while no tumors developed from Huh7-pRC and Huh7-IR-B spheroids.

Analysis of xenografted tumors showed that the number of CK19-positive cells detected by IHC was significantly increased in Huh7-IR-A tumors (Fig. 5c). The expression of *PROM1* and *CD44* was also increased in Huh7-IR-A tumors as assessed by RT-qPCR (Fig. 5d). Consistent with GSEA data obtained from gene expression profiles of Huh7-IR-A and Huh7-pRC spheres, several inflammation-related signatures were found to be robustly enriched in Huh7-IR-A tumors compared to Huh7-pRC tumors (Supplementary Fig. S5). These data were validated by performing RT-qPCR on a panel of genes from inflammatory signatures (*CXCL10*, *VCAM1*, *IRF1*, *IFITM3*, *STAT3*) in tumors with similar volumes (859 ± 128 mm^3, 955 ± 98 mm^3 and 622 ± 129 mm^3 for Huh7-pRC, Huh7-IR-A and Huh7-IR-B tumors, respectively) (Fig. 5e). There was also a strong correlation between the expression levels of these genes and IR-A among tumors from all three groups (Supplementary Table S5). These data led us to look for an association between *CXCL10* expression and *INSRA:INSRB* ratio in our collection of 85 human HCC. The mean value for *CXCL10* fold-change (T/NT) was higher in HCC with a high *INSRA:INSRB* ratio (10.7 ± 5.3 *vs* 6.3 ± 2.0-fold) but this did not reach significance.

3.5. IR-A overexpression increases aggressive features in HCC cells devoid of strong IGF-II autocrine loop

Human data showed that the upregulation of *INSRA*:*INSRB* ratio may exist in the absence of *IGF2* upregulation in HCC (Fig. 1d). Therefore, we examined whether IR-A overexpression could promote aggressive features in a HCC cell line devoid of strong IGF-II autocrine loop such as PLC/PRF5 cells (Supplementary S1). As shown in Fig. 6a, PLC/PRF5 cells overexpressing IR-A (PLC-IR-A) did not exhibit basal phosphorylation of IR-GFP and AKT but were responsive to exogenous insulin and IGF-II. PLC-IR-A cells had a higher invasion capacity than PLC-pRC and PLC-IR-B cells *in vitro* (Fig. 6b). In our hands, PLC/PRF5 cell lines showed grape-like morphology in non-adherent conditions which prevented an accurate quantification of spheroid numbers (Fig. 6c). None of the PLC cell lines expressed significant levels of *CK19* and *CD44* (data not shown). Nevertheless, PLC-IR-A spheres expressed increased *PROM1* and *AFP* mRNA levels compared to PLC-pRC and PLC-IR-B cells (Fig. 6d). After injection of 2×10^6 cells to nude mice, the delay for tumor appearance was similar between PLC/PFR5 cells overexpressing IR-A or IR-B (Fig. 6e and Supplementary Table S4). However, the growth of PLC-IR-B tumors was significantly slower than that of PLC-IR-A tumors (Fig. 6e and f and Supplementary Table S4). The induction of pro-inflammatory genes was observed in PLC-IR-A tumors while these genes were downregulated in PLC-IR-B tumors compared to controls (Fig. 6g). There was a strong correlation between IR-A and inflammatory gene mRNA levels in PLC/PRF5-derived tumors (Supplementary Table S5). Altogether, the data obtained with PLC/PRF5-derived cell lines corroborated those obtained with Huh7-derived cell lines and suggest that a strong IGF-II autocrine loop is not mandatory for the mediation of IR-A pro-tumorigenic effects.

4. Discussion

We report that *INSRA:INSRB* ratio was significantly more elevated in human HCC expressing stem/progenitor cell features such as CK19 and AFP and was associated with shorter patient survival after curative resection. The dysregulation of *INSRA:INSRB* ratio was more frequent than the upregulation of *IGF2* expression and was inversely correlated with the loss of *GRB14* indicating that the IR signaling pathway is deregulated at different levels in HCC.

To decipher the role of IR-A in HCC progression, we engineered new HCC cell lines with ectopic overexpression of IR-A or IR-B and performed a comprehensive *in vitro* and *in vivo* analysis. We choose this strategy because previous studies showed that the selective down-regulation of *INSRA* mRNA with siRNA was impossible to achieve in cancer cells [13,31,32]. Recently, we have developed a Crispr/Cas9 strategy to eliminate exon 11 in *INSR* gene to selectively express *INSRA* mRNA. Our preliminary results obtained in PLC/PRF5 cells support the present findings by showing that the reinforcement of IR-A expression to the detriment of IR-B confers higher aggressiveness to HCC cells (data not shown).

The presence of CSC markers in HCC has been postulated to be important in tumor initiation and progression, to be associated with high metastatic potential and chemotherapy resistance and to be predictive of poor outcome in patients [33]. We observed that the overexpression of IR-A up-regulated the expression of stemness-related

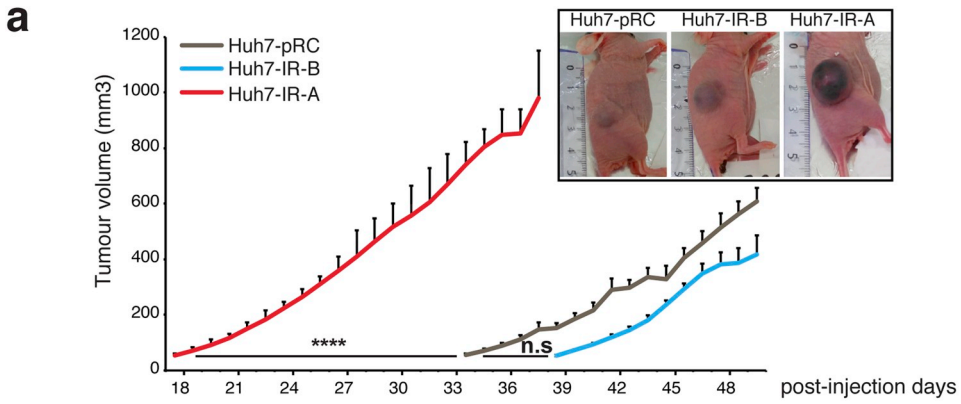

b

Cell lines	Mice with a tumor
Huh7-pRC	0/4
Huh7-IR-B	0/4
Huh7-IR-A	3/4*

*, one died prematurely from lymphoma

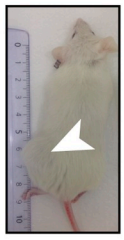

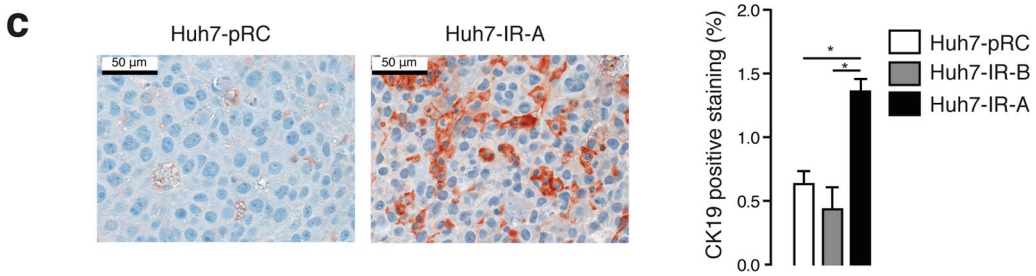

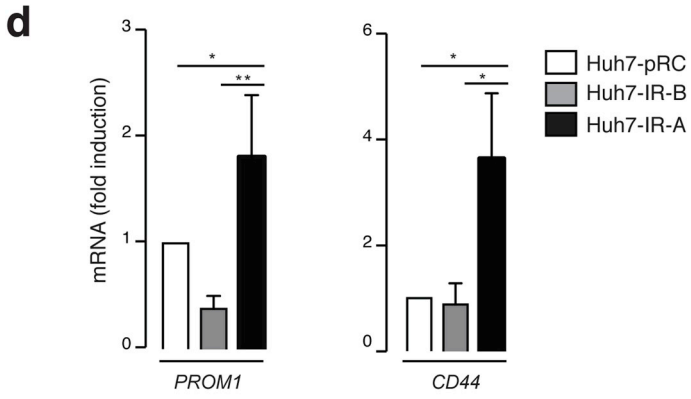

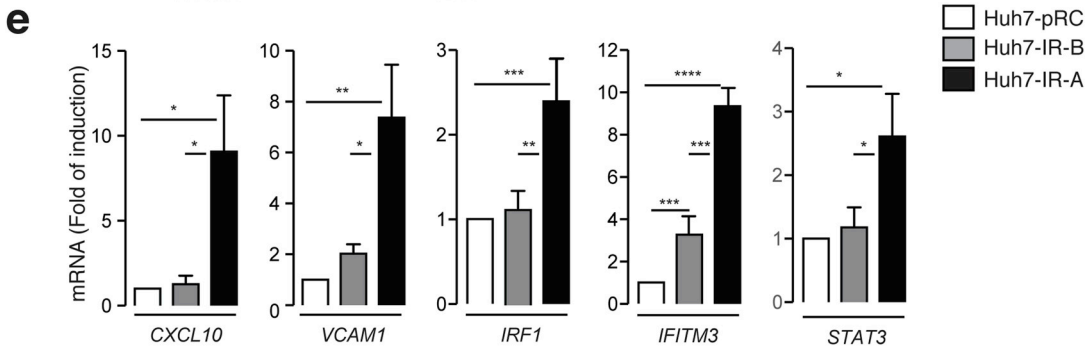

(caption on next page)

Fig. 5. Effects of IR-A overexpression on tumorigenicity of Huh7 cells *in vivo*. **a.** Tumor growth in nude mice subcutaneously injected with Huh7 cells stably expressing the empty plasmid (Huh7-pRC, n = 10), IR-A-GFP cDNA (Huh7-IR-A, n = 9), or IR-B-GFP cDNA (Huh7-IR-B, n = 5). *Inset*: Representative pictures of tumors 32 days after injection. **b.** 1×10^3 cells dissociated from Huh7-pRC, Huh7-IR-A and Huh7-IR-B hepatospheres were injected subcutaneously to NOD/SCID mice (n = 4 per group) and tumor development was followed over 6 months. A representative mouse having developed a tumor after injection of Huh7-IR-A hepatospheres is shown on the right. **c.** CK19 protein was detected by IHC in Huh7-pRC (n = 4) and Huh7-IR-A (n = 4) tumors. **d.** Expression of *PROM1* and *CD44* mRNA was measured by RT-qPCR in Huh7-pRC (n = 5), Huh7-IR-A (n = 5) and Huh7-IR-B (n = 4) tumors. **e.** Expression of *CXCL10, VCAM1, IRF1, IFITM3,* and *STAT3* mRNA was measured by RT-qPCR in Huh7-pRC (n = 5), Huh7-IR-A (n = 5) and Huh7-IR-B (n = 4) tumors. $*p < 0.05$, $**p < 0.01$, $***p < 0.001$, $****p < 0.0001$. ns, not significant.

genes in spheroids and xenografts. These findings suggest that IR-A acts on cell plasticity, promoting the retrodifferentiation of HCC cells into more immature hepatoblasts. The ability of cells derived from Huh7-IR-A but not from Huh7-pRC and Huh7-IR-B spheres to form tumors over 6 months in SCID mice also strengthens the hypothesis that this peculiar cellular contingent plays a prominent role in the tumorigenic process induced by IR-A. While EMT has been related to the promotion of cell motility and the acquisition of stem cell features, we did not find *in vitro* evidence for EMT induction upon enforced IR-A expression. However, GSEA showed a significant enrichment in an EMT signature in Huh7-IR-A-derived tumors (Supplementary Fig. S5).

Inflammation has been reported to promote the expansion of CSC contingent in HCC. For example, NF-κB is activated in aggressive HCCs and is associated with stemness features [29,34]. In the same way, tumor-associated macrophages produce interleukin-6 and signal *via* STAT3 to promote expansion of human HCC stem cells [35]. Therefore, the inflammatory gene program induced by sustained overexpression of IR-A in sphere-forming cells could favor the engagement of CSC *in vivo*. Among the most stimulated inflammation-related genes, *CXCL10* codes for a chemokine involved in the recruitment of immune cells and associated with HCC recurrence and poor survival [36]. CXCL10 and its receptor CXCR3 were reported to promote migration and invasion in HCC cell lines [37,38]. In our collection of HCC, *CXCL10* expression was higher in tumors with high *INSRA:INSRB* ratio but this was not significant. Further studies are required to better understand the role of inflammation pathways in IR-A mediated tumor progression.

Another important finding is that IR-A overexpression is able to drive oncogenic mechanisms in the presence or absence of a strong IGF-II autocrine loop. Endogenous IGF-II (Huh7 model) plays a contributory role in the promotion of IR-A-mediated cell aggressiveness since si-IGF2 inhibited IR-A induction of AKT signaling and invasion. In addition, IR-A overexpression had more pronounced effects on tumor onset and growth when overexpressed in Huh7 cells rather than in PLC/PRF5 cells in the xenograft model, suggesting that autocrine secretion of IGF-II boosted tumor growth. In the absence of IGF-II autocrine loop (PLC/PRF5 model), overexpressed IR-A might be activated by exogenous ligands provided by culture medium. *In vivo*, circulating IGF-II and/or insulin produced by the recipient animals may be efficient to stimulate IR-A-dependent signaling pathways in injected PLC-IR-A cells, thus circumventing the need for the cells to produce IGF-II.

IR-A has often been described as a mitogenic isoform in response to IGF-II binding, particularly in IGF1R-deficient cells [39]. While rather metabolic functions have been ascribed to IR-B in response to insulin, there is growing evidence that IR-B may also signal proliferation in response to insulin [7,31,40]. Here, we did not observe any influence of IR isoform overexpression on the *in vitro* proliferative ability of Huh7 and PLC/PRF5 cell lines. This may result from the fact that these cell lines expressed significant levels of IGF1R and were cultured in 10% fetal calf serum thus promoting the activation of concomitant and redundant proliferative pathways. In marked contrast, the proliferation of Huh7-IR-A and PLC-IR-A cells was enhanced after injection to nude mice suggesting that these cells have a better propensity to promote a permissive microenvironment for their proliferation *in vivo*. In this setting, inflammation could favor close communication between tumor cells and microenvironment contributing to tumor growth and aggressiveness.

In conclusion, our experimental data identify IR-A as a novel player of HCC progression, acting notably through the promotion of stem/progenitor cell features. These findings provide a molecular link to account for the association between high *INSRA:INSRB* ratio and CSC markers (such as CK19 and AFP) in human HCC. Moreover, the presence of an IGF-II autocrine loop is not a prerequisite for mediating the pro-tumorigenic function of IR-A. IR has been largely ignored as a possible target for years due to subsequent expectation of high toxicity. Accumulative evidence for the involvement of IR-A in the progression of different cancers including HCC should warrant further research to develop specific IR-A targeting strategies. In addition, the present results as well as our recent data showing a close correlation between the expression levels of *INSRA* mRNA in HCC tumors and the circulating levels of IR-A [8] suggest that soluble IR-A could be considered as a progression biomarker in HCC.

Conflict of interest

Nothing to declare.

Fundings

E. Benabou has been a fellow from Ligue Contre le Cancer (GB/MA/CD-11287). This work has been supported by grants from INSERM, GEFLUC, Ligue Contre le Cancer (Comité de Paris, RS17/75–93, RS18/75-85), Cancéropôle Ile de France and INCa (INCa-DGOS_5790).

Acknowledgements

We are deeply indebted to Corina Buta for expert technical assistance. We thank Dr Franck Peiretti (INSERM UMR_1062, Marseille) who provided us with IR expression plasmids, Annie Munnier (CISA, UMS_30 LUMIC, Paris) and Dr Romain Morrichon (imaging platform, CISA, INSERM UMR_S938) for their help in cytometry and microscopy analyses, respectively. We thank Sébastien Jacques, Angéline Duché and Franck Letourneur from the platform GENOM'IC (Cochin Institute, INSERM U1016, Paris) for microarray experiments, Tatiana Ledent and the staff of the animal facility of the Saint-Antoine Research Center (INSERM UMR_S938), and the histomorphology platform (UMS_30 LUMIC, Paris). We thank Dr Angélique Gougelet for critical reading of

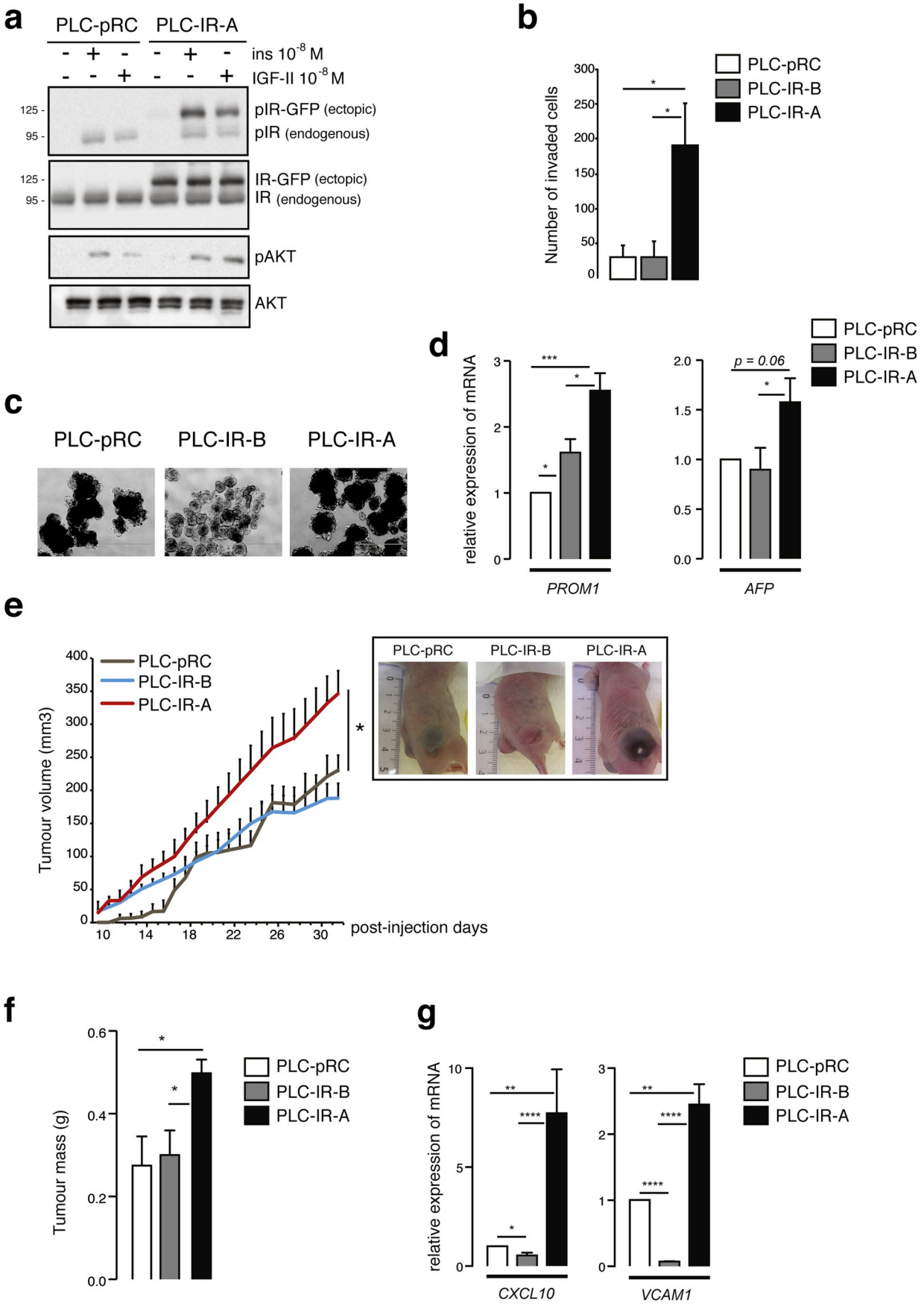

(caption on next page)

Fig. 6. Effects of IR-A overexpression on PLC/PRF5 cells properties. **a.** Western blot analysis of stably transfected PLC/PRF5 pools stimulated with or without insulin or IGF-II. Ectopic receptors fused to GFP (IR-GFP) have an apparent molecular weight of 125 kDa. **b.** Cell invasion was measured 30 h after plating using Transwell® inserts coated with Matrigel® (n = 7). **c.** Representative pictures showing morphology of spheroids. **d.** Expression of *PROM1 and AFP* mRNA was measured by RT-qPCR (n = 4). **e.** Tumor growth in nude mice *sc* injected with PLC/PRF5 cells stably expressing the empty plasmid (PLC-pRC, n = 10), IR-A-GFP cDNA (PLC-IR-A, n = 9), or IR-B-GFP cDNA (PLC-IR-B, n = 5). *Inset*: Representative pictures of tumors 32 days after injection. **f.** Tumor weight at sacrifice (n = 10, n = 9, and n = 5 for PLC-pRC, PLC-IR-A, and PLC-IR-B derived tumors, respectively). **g.** Expression of *CXCL10* and *VCAM1* mRNA was measured by RT-qPCR in PLC-pRC (n = 5), PLC-IR-A (n = 5) and PLC-IR-B (n = 4) tumors. *$p < 0.05$, **$p < 0.01$, ***$p < 0.001$, ****$p < 0.0001$.

the manuscript. We acknowledge the biobank CRB HUEP from AP-HP for access to human HCC samples.

Appendix A. Supplementary data

Supplementary data to this article can be found online at https://doi.org/10.1016/j.canlet.2019.02.037.

References

[1] G.B.D. Mortality, C. Causes of Death, Global, regional, and national age-sex specific all-cause and cause-specific mortality for 240 causes of death, 1990-2013: a systematic analysis for the Global Burden of Disease Study 2013, Lancet 385 (2015) 117–171.

[2] J.M. Llovet, J. Zucman-Rossi, E. Pikarsky, B. Sangro, M. Schwartz, M. Sherman, G. Gores, Hepatocellular carcinoma, Nat Rev Dis Primers 2 (2016) 16018.

[3] Z.M. Younossi, A.B. Koenig, D. Abdelatif, Y. Fazel, L. Henry, M. Wymer, Global epidemiology of nonalcoholic fatty liver disease-Meta-analytic assessment of prevalence, incidence, and outcomes, Hepatology 64 (2016) 73–84.

[4] F. Frasca, G. Pandini, P. Scalia, L. Sciacca, R. Mineo, A. Costantino, I.D. Goldfine, A. Belfiore, R. Vigneri, Insulin receptor isoform A, a newly recognized, high-affinity insulin-like growth factor II receptor in fetal and cancer cells, Mol. Cell Biol. 19 (1999) 3278–3288.

[5] A. Belfiore, R. Malaguarnera, V. Vella, M.C. Lawrence, L. Sciacca, F. Frasca, A. Morrione, R. Vigneri, Insulin receptor isoforms in physiology and disease: an updated view, Endocr. Rev. 38 (2017) 379–431.

[6] H. Chettouh, L. Fartoux, L. Aoudjehane, D. Wendum, A. Claperon, Y. Chretien, C. Rey, O. Scatton, O. Soubrane, F. Conti, F. Praz, C. Housset, O. Rosmorduc, C. Desbois-Mouthon, Mitogenic insulin receptor-A is overexpressed in human hepatocellular carcinoma due to EGFR-mediated dysregulation of RNA splicing factors, Cancer Res. 73 (2013) 3974–3986.

[7] L. Morzyglod, M. Cauzac, L. Popineau, P.D. Denechaud, L. Fajas, B. Ragazzon, V. Fauveau, J. Planchais, M. Vasseur-Cognet, L. Fartoux, O. Scatton, O. Rosmorduc, S. Guilmeau, C. Postic, C. Desdouets, C. Desbois-Mouthon, A.F. Burnol, Growth factor receptor binding protein 14 inhibition triggers insulin-induced mouse hepatocyte proliferation and is associated with hepatocellular carcinoma, Hepatology 65 (2017) 1352–1368.

[8] P.J. Meakin, S.M. Jalicy, G. Montagut, D.J.P. Allsop, D.L. Cavellini, S.W. Irvine, C. McGinley, M.K. Liddell, A.D. McNeilly, K. Parmionova, Y.R. Liu, C.L.S. Bailey, J.K. Dale, L.K. Heisler, R.J. McCrimmon, M.L.J. Ashford, Bace1-dependent amyloid processing regulates hypothalamic leptin sensitivity in obese mice, Sci. Rep. 8 (2018) 55.

[9] L. Sciacca, A. Costantino, G. Pandini, R. Mineo, F. Frasca, P. Scalia, P. Sbraccia, I.D. Goldfine, R. Vigneri, A. Belfiore, Insulin receptor activation by IGF-II in breast cancers: evidence for a new autocrine/paracrine mechanism, Oncogene 18 (1999) 2471–2479.

[10] V. Vella, G. Pandini, L. Sciacca, R. Mineo, R. Vigneri, V. Pezzino, A. Belfiore, A novel autocrine loop involving IGF-II and the insulin receptor isoform-A stimulates growth of thyroid cancer, J. Clin. Endocrinol. Metab. 87 (2002) 245–254.

[11] S. Avnet, L. Sciacca, M. Salerno, G. Gancitano, M.F. Cassarino, A. Longhi, M. Zakikhani, J.M. Carboni, M. Gottardis, A. Giunti, M. Pollak, R. Vigneri, N. Baldini, Insulin receptor isoform A and insulin-like growth factor II as additional treatment targets in human osteosarcoma, Cancer Res. 69 (2009) 2443–2452.

[12] L. Sciacca, R. Mineo, G. Pandini, A. Murabito, R. Vigneri, A. Belfiore, In IGF-I receptor-deficient leiomyosarcoma cells autocrine IGF-II induces cell invasion and protection from apoptosis via the insulin receptor isoform A, Oncogene 21 (2002) 8240–8250.

[13] I. Heidegger, J. Kern, P. Ofer, H. Klocker, P. Massoner, Oncogenic functions of IGF1R and INSR in prostate cancer include enhanced tumor growth, cell migration and angiogenesis, Oncotarget 5 (2014) 2723–2735.

[14] H. Zhang, A.M. Pelzer, D.T. Kiang, D. Yee, Down-regulation of type I insulin-like growth factor receptor increases sensitivity of breast cancer cells to insulin, Cancer Res. 67 (2007) 391–397.

[15] D.B. Ulanet, D.L. Ludwig, C.R. Kahn, D. Hanahan, Insulin receptor functionally enhances multistage tumor progression and conveys intrinsic resistance to IGF-1R targeted therapy, Proc. Natl. Acad. Sci. U. S. A 107 (2010) 10791–10798.

[16] E. Buck, P.C. Gokhale, S. Koujak, E. Brown, A. Eyzaguirre, N. Tao, M. Rosenfeld-Franklin, L. Lerner, M.I. Chiu, R. Wild, D. Epstein, J.A. Pachter, M.R. Miglarese, Compensatory insulin receptor (IR) activation on inhibition of insulin-like growth factor-1 receptor (IGF-1R): rationale for cotargeting IGF-1R and IR in cancer, Mol. Canc. Therapeut. 9 (2010) 2652–2664.

[17] C. Garofalo, M.C. Manara, G. Nicoletti, M.T. Marino, P.L. Lollini, A. Astolfi, G. Pandini, J.A. Lopez-Guerrero, K.L. Schaefer, A. Belfiore, P. Picci, K. Scotlandi, Efficacy of and resistance to anti-IGF-1R therapies in Ewing's sarcoma is dependent on insulin receptor signaling, Oncogene 30 (2011) 2730–2740.

[18] D. Weinstein, R. Sarfstein, Z. Laron, H. Werner, Insulin receptor compensates for IGF1R inhibition and directly induces mitogenic activity in prostate cancer cells, Endocr Connect 3 (2014) 24–35.

[19] I. Martinez-Quetglas, R. Pinyol, D. Dauch, S. Torrecilla, V. Tovar, A. Moeini, C. Alsinet, A. Portela, L. Rodriguez-Carunchio, M. Sole, A. Lujambio, A. Villanueva, S. Thung, M. Esteller, L. Zender, J.M. Llovet, IGF2 is up-regulated by epigenetic mechanisms in hepatocellular carcinomas and is an actionable oncogene product in experimental models, Gastroenterology 151 (2016) 1192–1205.

[20] C. Goumard, C. Desbois-Mouthon, D. Wendum, C. Calmel, F. Merabtene, O. Scatton, F. Praz, Low levels of microsatellite instability at simple repeated sequences commonly occur in human hepatocellular carcinoma, CANCER GENOMICS PROTEOMICS 14 (2017) 329–339.

[21] M.J. Blivet-Van Eggelpoel, H. Chettouh, L. Fartoux, L. Aoudjehane, V. Barbu, C. Rey, S. Priam, C. Housset, O. Rosmorduc, C. Desbois-Mouthon, Epidermal growth factor receptor and HER-3 restrict cell response to sorafenib in hepatocellular carcinoma cells, J. Hepatol. 57 (2012) 108–115.

[22] B. Leibiger, I.B. Leibiger, T. Moede, S. Kemper, R.N. Kulkarni, C.R. Kahn, L.M. de Vargas, P.O. Berggren, Selective insulin signaling through A and B insulin receptors regulates transcription of insulin and glucokinase genes in pancreatic beta cells, Mol. Cell 7 (2001) 559–570.

[23] S. Uhles, T. Moede, B. Leibiger, P.O. Berggren, I.B. Leibiger, Isoform-specific insulin receptor signaling involves different plasma membrane domains, J. Cell Biol. 163 (2003) 1327–1337.

[24] R.R. Ramos, A.J. Swanson, J. Bass, Calreticulin and Hsp90 stabilize the human insulin receptor and promote its mobility in the endoplasmic reticulum, Proc. Natl. Acad. Sci. U. S. A. 104 (2007) 10470–10475.

[25] I. Kara, M. Poggi, B. Bonardo, R. Govers, J.F. Landrier, S. Tian, I. Leibiger, R. Day, J.W. Creemers, F. Peiretti, The paired basic amino acid-cleaving enzyme 4 (PACE4) is involved in the maturation of insulin receptor isoform B: an opportunity to reduce the specific insulin receptor-dependent effects of insulin-like growth factor 2 (IGF2), J. Biol. Chem. 290 (2015) 2812–2821.

[26] A. Nagarajan, M.C. Petersen, A.R. Nasiri, G. Butrico, A. Fung, H.B. Ruan, R. Kursawe, S. Caprio, J. Thibodeau, M.C. Bourgeois-Daigneault, L. Sun, G. Gao, S. Bhanot, M.J. Jurczak, M.R. Green, G.I. Shulman, N. Wajapeyee, MARCH1 regulates insulin sensitivity by controlling cell surface insulin receptor levels, Nat. Commun. 7 (2016) 12639.

[27] C. Buta, E. Benabou, M. Lequoy, H. Regnault, D. Wendum, F. Meratbene, H. Chettouh, L. Aoudjehane, F. Conti, Y. Chretien, O. Scatton, O. Rosmorduc, F. Praz, L. Fartoux, C. Desbois-Mouthon, Heregulin-1b and HER3 in hepatocellular carcinoma: status and regulation by insulin, J. Exp. Clin. Cancer Res. 35 (2016) 126.

[28] A. Subramanian, P. Tamayo, V.K. Mootha, S. Mukherjee, B.L. Ebert, M.A. Gillette, A. Paulovich, S.L. Pomeroy, T.R. Golub, E.S. Lander, J.P. Mesirov, Gene set enrichment analysis: a knowledge-based approach for interpreting genome-wide expression profiles, Proc. Natl. Acad. Sci. U. S. A. 102 (2005) 15545–15550.

[29] J.U. Marquardt, L. Gomez-Quiroz, L.O. Arreguin Camacho, F. Pinna, Y.H. Lee, M. Kitade, M.P. Dominguez, D. Castven, K. Breuhahn, E.A. Conner, P.R. Galle, J.B. Andersen, V.M. Factor, S.S. Thorgeirsson, Curcumin effectively inhibits oncogenic NF-kappaB signaling and restrains stemness features in liver cancer, J. Hepatol. 63 (2015) 661–669.

[30] R. Portillo-Lara, M.M. Alvarez, Enrichment of the cancer stem phenotype in sphere cultures of prostate cancer cell lines occurs through activation of developmental pathways mediated by the transcriptional regulator DeltaNp63alpha, PLoS One 10 (2015) e01x30118.

[31] C.M. Perks, H.A. Zielinska, J. Wang, C. Jarrett, A. Frankow, M.R. Ladomery, A. Bahl, A. Rhodes, J. Oxley, J.M. Holly, Insulin receptor isoform variations in prostate cancer cells, Front. Endocrinol. 7 (2016) 132.

[32] C. Berlato, W. Doppler, Selective response to insulin versus insulin-like growth factor-I and -II and up-regulation of insulin receptor splice variant B in the differentiated mouse mammary epithelium, Endocrinology 150 (2009) 2924–2933.

[33] D. Sia, A. Villanueva, S.L. Friedman, J.M. Llovet, Liver cancer cell of origin, molecular class, and effects on patient prognosis, Gastroenterology 152 (2017) 745–761.

[34] H. Dubois-Pot-Schneider, K. Fekir, C. Coulouarn, D. Glaise, C. Aninat, K. Jarnouen, R. Le Guevel, T. Kubo, S. Ishida, F. Morel, A. Corlu, Inflammatory cytokines promote the retrodifferentiation of tumor-derived hepatocyte-like cells to progenitor cells, Hepatology 60 (2014) 2077–2090.

[35] S. Wan, E. Zhao, I. Kryczek, L. Vatan, A. Sadovskaya, G. Ludema, D.M. Simeone, W. Zou, T.H. Welling, Tumor-associated macrophages produce interleukin 6 and signal via STAT3 to promote expansion of human hepatocellular carcinoma stem cells, Gastroenterology 147 (2014) 1393–1404.

[36] C.X. Li, C.C. Ling, Y. Shao, A. Xu, X.C. Li, K.T. Ng, X.B. Liu, Y.Y. Ma, X. Qi, H. Liu, J. Liu, O.W. Yeung, X.X. Yang, Q.S. Liu, Y.F. Lam, Y. Zhai, C.M. Lo, K. Man,

CXCL10/CXCR3 signaling mobilized-regulatory T cells promote liver tumor recurrence after transplantation, J. Hepatol. 65 (2016) 944–952.
[37] Y. Qin, S.Q. Xu, D.B. Pan, G.X. Ye, C.J. Wu, S. Wang, C.J. Wang, J.Y. Jiang, J. Fu, Silencing of WWP2 inhibits adhesion, invasion, and migration in liver cancer cells, Tumour Biol. 37 (2016) 6787–6799.
[38] T. Ren, L. Zhu, M. Cheng, CXCL10 accelerates EMT and metastasis by MMP-2 in hepatocellular carcinoma, Am. J. Transl. Res. 9 (2017) 2824–2837.
[39] A. Belfiore, F. Frasca, G. Pandini, L. Sciacca, R. Vigneri, Insulin receptor isoforms and insulin receptor/insulin-like growth factor receptor hybrids in physiology and disease, Endocr. Rev. 30 (2009) 586–623.
[40] G. Pandini, F. Frasca, R. Mineo, L. Sciacca, R. Vigneri, A. Belfiore, Insulin/insulin-like growth factor I hybrid receptors have different biological characteristics depending on the insulin receptor isoform involved, J. Biol. Chem. 277 (2002) 39684–39695.